

# Convex Formulations of Air Traffic Flow Optimization Problems

*A new technique for modeling changes in overall traffic flow increases the feasibility of maximizing aircraft arrivals and minimizing delays.*

By DANIEL B. WORK, *Student Member IEEE*, AND ALEXANDRE M. BAYEN, *Member IEEE*

**ABSTRACT** | The problem of regulating air traffic in the en route airspace of the National Airspace System is studied using a Eulerian network model to describe air traffic flow. The evolution of traffic on each edge of the network is modeled by a modified Lighthill-Whitham-Richards partial differential equation. The equation is transformed with a variable change, which makes it linear and enables us to use linear finite difference schemes to discretize the problem. We pose the problem of optimal traffic flow regulation as a continuous optimization program in which the partial differential equation appears in the constraints. We propose a discrete formulation of this problem, which makes all constraints (the discretized partial differential equations, boundary, and initial conditions) linear. Corresponding linear programming and quadratic programming based solutions to this convex optimization program yield globally optimal solutions to various air traffic management objectives. The proposed method is applied to the maximization of aircraft arrivals and minimization of delays in the arrival airspace due to exogenous capacity reductions. The corresponding linear and quadratic programs are solved numerically using CPLEX for a benchmark scenario in the Oakland Air Route Traffic Control Center. Several computational aspects of the method are assessed—in particular, accuracy of the numerical discretization, computational time, and storage space required by the method.

**KEYWORDS** | Convex optimization; finite differences; partial differential equations

Manuscript received November 4, 2007; revised August 27, 2008. Current version published January 16, 2009.

The authors are with Systems Engineering, Department of Civil and Environmental Engineering, University of California, Berkeley, CA 94720 USA (e-mail: dbwork@berkeley.edu; bayen@berkeley.edu).

Digital Object Identifier: 10.1109/JPROC.2008.2006150

## I. INTRODUCTION

### A. General Motivation

The number of airborne aircraft in the continental U.S. airspace exceeds 5000 on a daily basis [7]. Over the last 40 years, air traffic has increased by 50% [27], and the total number of passenger miles traveled on commercial airlines is expected to grow from a record 741 million in 2006 to more than 1 billion by 2015 [14] in the United States alone. To help coordinate flight paths and ensure safety, a hierarchy of control systems was developed for the *National Airspace System* (NAS). Starting at the top of the hierarchy is a single *Air Traffic Control System Command Center* (ATCSCC), which supervises overall traffic and 22 *air route traffic control centers* (ARTCCs). Within each ARTCC are approximately 20 high-altitude sectors (or sectors, for brevity), each controlled by one or multiple air traffic controllers. Air traffic controllers communicate directly with each aircraft in their sector to guide their flight. Coordination between the different sectors is achieved using *Federal Aviation Administration* (FAA) standards. As the volume of traffic continues to grow, new control strategies need to be developed that can minimize delays and increase the overall throughput capacity of the system.

### B. Aggregate Models for Air Traffic Management

Research on the steady increase in air traffic volume has triggered the development of a new class of *aggregate* flow models, which describe the evolution of flows of aircraft rather than individual trajectories in the hope of capturing traffic patterns in a tractable manner. By employing such a strategy, a significant order reduction in model complexity can be achieved. The goal of these models is therefore to generate aggregate control strategies that reproduce single aircraft controls as closely as possible while maintaining tractability.

Reference [23] was to our best knowledge the first to define traffic flow using an *Eulerian*, or control volume based, framework. This work uses a discretized version of the *Lighthill–Whitham–Richards* (LWR) *partial differential equation* (PDE) [19], [33] and is motivated by the Daganzo cell transmission model [12], [13] in a particular flow regime called “free flow.” This work has since inspired several research groups to generate similar models using a stochastic framework [34], [36]. Two-dimensional models [24] have also emerged, in the hope of capturing traffic flow patterns more precisely. An important characteristic of these approaches [23], [24], [34], [36] is the diffusion or dispersion that they exhibit. While this is not a problem in a stochastic framework (since the results are in the expected sense), it is more problematic in deterministic models such as [23] and [24], since this potentially leads to aircraft losses or inaccurate predictions (this fact has been reported in the literature [4]).

A first attempt to resolve these issues was proposed in the form of a continuous time/continuous space model in earlier work of one of the authors [4], based directly on the LWR PDE. While this approach solves the diffusion problem, its computational tractability could be improved (it depends on the required space discretization), and the resulting optimization programs require heavy computations based on adjoint problems [39]. More recently, a two-level control system for optimal traffic flow management was developed [26], in which an inner-level control module takes in the optimal inflow and outflow commands generated by an outer control module as reference inputs and uses hybrid aircraft models to search for optimal trajectories.

Reference [39] proposes a *large-capacity cell transmission model* [CTM(L)] based on a graph-theoretic network flow model constructed from historical traffic data. The model consists of a linear time-invariant dynamical system used for optimization of traffic flow. In [40], the authors compare the predictive capabilities of the CTM(L) with three other Eulerian models, including the model used in this paper: the *PDE model* [4], *modified Menon model* (MMM) [23], and *two-dimensional Menon model* (2DMM) [24]. The PDE model is an extension of the LWR PDE to a network of high-altitude air traffic routes. The MMM is an extension of [23], in which air traffic is spatially aggregated into control volumes on one-dimensional line segments. The 2DMM partitions the airspace into two-dimensional control volumes, each with up to nine streams passing through it. The streams represent directions that aircraft may travel through the control volume, and model parameters determine how aircraft switch from one stream to another within the control volume.

The analysis presented in [40] is significant because each of the four models is benchmarked on the same network for a fair comparison between the different models. The strength of the PDE model is its predictive performance, as it simulates air traffic with the least error of the four models. The accuracy of the PDE model comes at a high

computational expense when presented in an optimization framework because it is nonlinear in its decision variables. The discrete CTM(L) model, which has reasonable accuracy but is nearly ten times faster than the continuous PDE model (in terms of computational time), appears to strike a reasonable balance between accuracy and efficiency.

The contribution of this paper is to improve the computational cost of the optimization problem based on the PDE model, which has previously been its biggest weakness. We introduce a new convex formulation of the PDE model and discretize it, resulting in a new ATM optimization framework that can be solved efficiently using standard *linear programming* (LP) or *quadratic programming* (QP) techniques. This new formulation also provides a certificate that the resulting control policy is globally optimal, which is not true for many optimization techniques applied to the nonconvex models such as the CTM(L) model or the non-convex form of the PDE model used in [4].

### C. Control of Partial Differential Equation Driven Systems

Each of the Eulerian models mentioned above can be used to develop flow control strategies at a NAS-wide level. The specificity of the model presented in this paper is its formulation as a PDE driven model. Control and optimization of systems driven by PDEs is a vast field, for which numerous solution methods have been developed. A standard way of achieving these NAS-wide control strategies is to pose the corresponding problems as optimization programs with an objective of maximizing the inflow into a destination airport, subject to bounds on the aircraft speed and the density of aircraft in a region, and a constraint that the flow must adhere the network model. Other techniques have alternately been applied to the control of such systems and models. For example, the Menon model [23] uses a state-space representation, and methods from linear system theory can be used for its analysis and control. In [39], the authors show that the problem of minimizing overall aircraft delay subject to peak aircraft count constraints can be formulated as an *integer linear program* (ILP) and solved by relaxing the integer constraint.

Within the suite of methods developed to control PDE driven systems, one possible approach to the problem of controlling or optimizing systems driven by PDEs is to work on a discretization of the PDE directly. This is the approach chosen in this paper. For example, in hydraulics, this approach has been applied successfully to the *Saint-Venant equations* (SVEs): in [1] and [22], an irrigation canal system is controlled by discretizing the SVEs to obtain a state-space model, which is then optimized to minimize the system’s response to uncertain water withdraws from the main flow in the canal.

Several additional techniques applied to PDE driven systems need to be mentioned here for completeness. An extensive overview of modeling and optimization of transportation networks modeled by PDEs can be found in the

recent book of Piccoli and Garavello [28] and can be used for the study of highway traffic flow. A variety of techniques exist for optimization of physical networks as well. Frequency-domain approaches have been used by Litrico *et al.* in the context of canal network control for the SVEs [20] and provide useful control techniques when underlying equations of flows are linear. Linear quadratic optimal control theory was applied by Malaterre for the automatic control of two different eight-pool irrigation canals [21]. Several approaches have been developed to handle nonlinear phenomena present in physical networks. A nonlinear output feedback method was studied in [2] for a compartmental network flow system. Methods based on Lyapunov analysis were presented by Coron *et al.* for a hydraulic application, namely, the level and flow regulation in a horizontal open channel [10]. A decentralized nonlinear control approach was used in [18] for fluid flow networks, where actuator valves and flow rate sensors are collocated in individual branches and do not exchange information. A similar model was used for optimal control of supply networks in [17].

While the list above outlines a variety of possible approaches to solve specific problems, one method stands out because of its generality. One of the most powerful techniques used for solving problems posed as optimization programs in which constraints appear in the form of PDEs is adjoint-based optimization [16]. This framework is very general and enables systematic treatment of cost functions and constraints. Its power is reflected by the variety of application fields in which it has been used—in particular, shape optimization [16], oceanography [5], river hydraulics [35], systems biology [29], optimal control of hybrid systems [30], and optimal control of transportation networks [30], [40]. While this method is very general and can be applied to almost any problem (including the present one), it has two main drawbacks: i) it does not provide any guarantee of global optimality and ii) it is computationally expensive, due to the necessity of sequentially solving a series of “direct” and “adjoint” problems and using iterative descent methods such as the *Broyden–Fletcher–Goldfarb–Shanno* (BFGS) method to optimize the cost [41]. While the BFGS method is efficient for small-scale problems, it becomes quite impractical when dealing with large-scale systems for which the cost of manipulating the Hessian approximations is too elevated. These two drawbacks are addressed in this paper by our proposed convex formulation of the problem.

#### D. Towards a Convex Optimization Framework

In this paper, we use a PDE model describing the evolution of cumulative aircraft count and density, which follow standard frameworks available in the transportation engineering literature. We choose to work with the PDE model because it has been shown to accurately predict the aircraft count in each sector during forward simulation, and the relevance of the model increases with the number of aircraft [40]. These two factors provide a motivation for our

use of this model as a basis for the optimization framework described later. When the velocity is prescribed (as is the case of forward model simulation), this model is a linear advection equation, which can be solved efficiently using nonlinear discretization schemes. However, if the model is encoded as a constraint in an optimization problem for which both the velocity and density are unknown, the resulting problem is nonlinear, even if linear discretization schemes are used. This has been treated previously by applying optimization techniques such as the adjoint method, which can handle the nonlinearities, at the expense of computational efficiency and global optimality of the solution.

After formally stating the constraints of the optimal control problem in the density and velocity decision variables, we show that a change of variables to density and flux will result in linear constraints in continuous form. If the PDE in this alternate form is discretized using linear discretization schemes, the resulting constraints are also linear, which is the key step to making the formulation convex. To complete the transformation into a convex optimization problem, we illustrate this technique on three different objective functions including maximizing the airspace throughput (i.e., the number of aircraft arriving at their destinations) and minimizing the changes to flight paths or arrival schedules caused by reduced network capacity.

From a purely theoretical standpoint, this is a significant step forward for determining optimal control strategies for the NAS because the resulting control policies are globally optimal. When earlier models [Menon, CTM(L) and even previous forms of the PDE model] are used for computing optimal ATM policies, the corresponding optimization problems have mixed integer decision variables or other nonlinearities, which destroy the problem’s convexity. The same is true for the mixed ILP framework presented in [6]. Thus, any optimal strategy computed from these models may only be locally optimal unless computationally costly branching techniques are introduced. In addition to providing a globally optimal solution, the convexity allows us to use very efficient optimization tools such as LP or QP to solve large-scale problems.

Even though the resulting formulation presented in this paper is convex, a proper discretization of the networked PDE problem is required to compute optimal speed policies. Through extensive numerical simulation, we have identified two problematic areas that prevent the blind application of any linear finite difference numerical scheme. With some care, an appropriate scheme can be selected that is feasible and corresponds to the physics described in the continuous convex PDE framework, with significant reductions in computational time.

The contributions of this paper thus include the following.

- A new continuous formulation of the nonlinear optimization program presented in [4], as a convex optimization program.
- The instantiation of several linear finite difference schemes on the present PDE to pose the previous

problem as a set of (discretized) convex programs of various forms, in the hope of finding the most efficient of them.

- A systematic study of the respective performance of these formulations. In particular, a choice of the numerical scheme is made, so that the convex optimization program provides appropriate solutions. In particular, we select schemes that avoid two major problems inherent to these types of convex optimization program formulations. i) These problems can become infeasible because of numerical overshoot/undershoot inherently present in finite difference schemes. ii) They can return physically meaningless “sawtooth-like” solutions due to features of the numerical discretization schemes, which are exploited by the optimization solver.
- A numerical study of their computational performance. We numerically validate the fact that they return globally optimal solutions, as predicted by theory. We show drastic improvements in computational time with respect to our earlier formulation, bringing the computational time from minutes [4] to seconds.
- An implementation of the program for a benchmark air traffic control problem for the en route arrival airspace in the Oakland center.

The remainder of this paper is organized as follows. In Section II, we present the PDE network model used to describe traffic flow, pose the general form of the optimization program, and discuss its transformation into an LP or QP form. A variety of finite difference schemes are subsequently introduced, and their suitability in terms of accuracy to the PDE model and computation time is compared in Section III. Common pitfalls that can occur when implementing these convex optimization programs are described in Section IV, and a final selection of a numerical scheme is made. The feasibility of the method is demonstrated on the Oakland ARTCC in Section V using arrival traffic benchmark scenarios.

## II. PROBLEM FORMULATION

### A. PDE Network Model

In this paper, we use the PDE model of air traffic flow initiated in [4], and later extended in [40]. This approach models jetways as paths composed of a series of line segments known as links, which range between 30 and 200 mi in length. In previous work, 13 742 trajectories across the NAS were reduced to build a network of 1598 links [40], a subset of which is used in this paper.

We represent each link  $k$  on a path as a segment  $[0, L]$  and denote by  $u(x, t)$  the number of aircraft between distances zero and  $x$  at time  $t$ . In particular,  $u(0, t) = 0$  and  $u(L, t)$  is the total number of aircraft in the path modeled by  $[0, L]$  at time  $t$ . In this paper, we assume a time-varying

velocity profile  $v(x, t) > 0$ , which represents the aggregate velocity of aircraft flow at position  $x$  and time  $t$ . Applying the conservation of mass to a control volume comprised between positions  $x$  and  $x + h$ , and letting  $h$  tend to zero, the following relation between the spatial and temporal derivatives of  $u(x, t)$  is obtained [4]

$$\begin{cases} \frac{\partial u(x,t)}{\partial t} + v(x,t) \frac{\partial u(x,t)}{\partial x} \\ \quad = v(0,t) \frac{\partial u(0,t)}{\partial x} & (x,t) \in (0,L) \times (0,T] \\ u(x,0) = u_{t_0}(x) & x \in [0,L] \\ u(0,t) = 0 & t \in [0,t] \end{cases} \quad (1)$$

where the term  $v(0,t)(\partial u(0,t)/\partial x)$  represents a prescribed rate at which aircraft enter the link (at  $x = 0$ ). We introduce the density of aircraft  $\rho(x, t)$  as the weak derivative of  $u(x, t)$  with respect to  $x$   $\rho(x, t) = (\partial u(x, t)/\partial x)$ , so that the evolution of aircraft density is a solution of the partial differential equation

$$\begin{cases} \frac{\partial \rho(x,t)}{\partial t} + v(x,t) \frac{\partial \rho(x,t)}{\partial x} \\ \quad + \frac{\partial v(x,t)}{\partial x} \rho(x,t) = 0 & (x,t) \in (0,L) \times (0,T] \\ \rho(x,0) = \rho_{t_0}(x) & x \in [0,L] \\ \rho(0,t) = \rho_{x_0}(t) & t \in [0,T] \end{cases} \quad (2)$$

with initial and boundary conditions  $\rho_{t_0}(x)$  and  $\rho_{x_0}(t)$ . This PDE is a linear advection equation with positive velocity and a source term  $(\partial v(x, t)/\partial x)\rho(x, t)$ . Clearly, the two systems (1) and (2) are equivalent and model the same physical phenomenon. Note that while (2) is linear in the state  $\rho(x, t)$ , if  $v(x, t)$  is also introduced as an unknown parameter to be determined by the optimization program, (2) becomes nonlinear when considered as a constraint.

This model of air traffic flow on a link can be extended to a network of links. We let  $\mathbb{K}$  denote the set of all links in the network. For each link  $k \in \mathbb{K}$ , we associate the set  $\mathbb{M}_k$  with the set of all links in the network in which flow merges into link  $k$ . We represent the portion of flow exiting link  $m \in \mathbb{M}_k$  that enters link  $k$  by  $\beta_{m,k}$ , where  $0 \leq \beta_{m,k} \leq 1$ . Because flow exiting  $m$  may split onto multiple links including  $k$ , we require that for a fixed  $m$ ,  $\sum_{i \in \mathbb{K}} \beta_{m,i} = 1$ . That is, the flow exiting from link  $m$  and diverging to all other links  $i$  must be conserved. For the simple network shown in Fig. 1, we have  $\mathbb{K} := \{1, \dots, 5\}$ ,  $\mathbb{M}_4 = \mathbb{M}_5 = \{1, 2, 3\}$ , and  $\beta_{m,4} + \beta_{m,5} = 1$ ,  $m \in \{1, 2, 3\}$ . The system of partial differential equations on a general network can be written as shown in the equation at the bottom of the next page. The well-posedness of (3), and the existence and uniqueness of the solution on the network, is proved in [40].

### B. Optimal Control Problem

With the PDE model defined above, we now pose the problems of maximizing the network throughput and

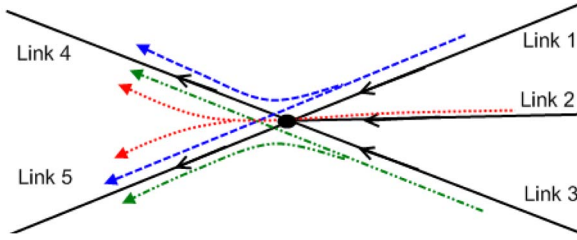


**Fig. 1. Simple example network composed of five links. The flow from links 1 (dashed blue), 2 (dotted red), and 3 (dash-dot green) each split and feed links 4 and 5.**

minimizing delays in the en route and arrival airspace as optimal control problems. In other words, we seek to find the globally optimal velocity profiles  $v_k(x, t)$  with respect to some network performance metric, for all links in the system. The novelty of this work is that unlike previous treatments of these optimal control problems, we do not solve for the velocity profile directly. Instead, we introduce a new formulation in which the velocity is computed from the optimal density and flux solutions. The most important contribution of this paper is that with this change of variables, the PDE network optimal control problem can be posed as a convex optimization problem, subsequently enabling globally optimal solutions which can be computed using efficient and well-developed LP or QP techniques.

1) *Constraints*: Following standard optimal control terminology, we encode the dynamics of the system in the form of constraints [8]. The key constraint in the optimization program is thus the constitutive model equation given in the form of PDEs of the  $\rho_k(x, t)$  functions. This also includes a prescribed initial density distribution  $\rho_{t_0, k}(x)$ , which represents the aircraft initially airborne. The conditions at the boundaries of each link  $\rho_k(0, t)$  are defined by aircraft entering the network from international flights or lower altitude traffic  $\rho_{x_0, k}(t)$  and aircraft entering from other links in the network. We impose upper and lower bounds on the velocity profile on each link  $v_{k, \min}(x, t) \leq v_k(x, t) \leq v_{k, \max}(x, t)$  to keep traffic flow consistent with the physical capabilities of the aircraft in the NAS.

An upper bound on the density on each link  $\rho_k(x, t) \leq \rho_{k, \max}(x, t)$  is added for two reasons. First, the FAA has established a minimum horizontal separation distance between aircraft in the en route environment of

five nautical miles. By imposing an upper bound on the density, we capture the essence of this requirement in an aggregated form, following the work in the field of Eulerian models [3], [4], [23], [24], [31], [32], [34], [36], [40]. Secondly, if air traffic controllers are used to dispatch the optimal control strategy to the pilots, the integral of the upper bound on the density corresponds to the maximal number of aircraft in a sector that the air traffic controller can legally handle. We also require the density to be nonnegative to be physically meaningful.

2) *Transformation of the Problem Into a Convex Optimization Program*: If these constraints are imposed along with the network PDE model, the optimization program for a single junction becomes

$$\begin{aligned}
 \min : & J \\
 \text{st} : & 0 \leq \rho_k(x, t) \leq \rho_{k, \max}(x, t) \\
 & (x, t) \in [0, L_k] \times [0, T], k \in \mathbb{K} \\
 & v_{k, \min}(x, t) \leq v_k(x, t) \leq v_{k, \max}(x, t) \\
 & (x, t) \in [0, L_k] \times [0, T], k \in \mathbb{K} \\
 & (3).
 \end{aligned} \tag{4}$$

The goal of the optimization problem is to find the optimal  $v_k(\cdot, \cdot)$  such that the objective function  $J$  is minimized. The output of this program is thus an optimal speed control policy to be applied by the air traffic controller.

The principle difficulty with solving (4) is that the PDE is a nonlinear constraint in the optimization variables, as was mentioned earlier. Thus, even if linear discretization schemes are used, the resulting constraints will be nonlinear. In the past, standard PDE optimization techniques such as adjoint methods have been used to solve these types of problems [4], [16], [31], [32], [35]. As explained earlier, the benefit of these methods is their generality. The drawbacks are the difficulty to implement them (using BFGS routines [41]), the lack of guarantees of numerical convergence and subsequent degree of suboptimality, and, in practice, the high computational cost of the resulting algorithms. In particular, recent work on second-order methods [32] displayed improved convergence to suboptimal values of first-order methods, which also underlines the lack of global certificates of optimality for this general class of methods (the performance of the second order method is so superior to the performance of

$$\begin{cases} \frac{\partial \rho_k(x, t)}{\partial t} + v_k(x, t) \frac{\partial \rho_k(x, t)}{\partial x} + \frac{\partial v_k(x, t)}{\partial x} \rho_k(x, t) = 0 & (x, t) \in (0, L_k) \times (0, T], k \in \mathbb{K} \\ \rho_k(x, 0) = \rho_{t_0, k}(x) & x \in [0, L_k], k \in \mathbb{K} \\ \rho_k(0, t) = \rho_{x_0, k}(t) + \frac{\sum_{m \in \mathbb{M}_k} \beta_{m, k} \rho_m(L_m, t) v(L_m, t)}{v_k(0, t)} & t \in [0, T], k \in \mathbb{K} \end{cases} \tag{3}$$

the first-order method that it emphasizes the suboptimality of the latter very strikingly).

We now propose a change of decision variables that makes the previous constraints in (4) linear

$$q_k(x, t) = \rho_k(x, t)v_k(x, t) \quad (5)$$

where  $q_k(x, t)$  is known as the flux function and can be interpreted as the amount of aircraft that flow through a point  $x$  on the link per unit time at time  $t$ . The nonlinear constraint in terms of decision variables  $\rho_k(x, t)$  and  $v_k(x, t)$  can be transformed into a linear constraint in terms of decision variables  $\rho_k(x, t)$  and  $q_k(x, t)$ . The control variable  $v_k(x, t)$  is completely absent in the resulting formulation, and so it must be computed from the optimal solutions for density and flux obtained by solving the following equivalent continuous optimization problem:

$$\begin{aligned} \min : & J \\ \text{st} : & 0 \leq \rho_k(x, t) \leq \rho_{\max}(x, t) \\ & (x, t) \in [0, L_k] \times [0, T], k \in \mathbb{K} \\ & v_{k, \min}(x, t)\rho_k(x, t) \leq q_k(x, t) \\ & \leq v_{k, \max}(x, t)\rho_k(x, t) \\ & (x, t) \in [0, L_k] \times [0, T], k \in \mathbb{K} \\ & \frac{\partial \rho_k(x, t)}{\partial t} + \frac{\partial q_k(x, t)}{\partial x} = 0 \\ & (x, t) \in (0, L_k) \times (0, T], k \in \mathbb{K} \\ & \rho_k(x, 0) - \rho_{t_0, k}(x) = 0 \\ & x \in [0, L_k], k \in \mathbb{K} \\ & q_k(0, t) - q_{x_0, k}(t) \\ & - \sum_{m \in \mathbb{M}_k} \beta_{m, k} q_m(L_m, t) = 0 \\ & t \in [0, T], k \in \mathbb{K}. \end{aligned} \quad (6)$$

Note also that the velocity constraint changed from bounds on  $v_k(x, t)$  in (4) to a linear constraint on  $q_k(x, t)$  and  $\rho_k(x, t)$  in (6). In this latter form, any linear discretization scheme will yield a discrete convex formulation that can be solved using either LP or QP techniques given an appropriate choice of the objective function and its discretization, or general convex optimization techniques if the objective function  $J$  is a general convex function.

3) *Objective Functions*: In order to pose convex objective functions, we introduce a single airport  $\alpha$  in the set of all airports  $\mathbb{A}$  in the network. If we wish to denote the number of arrivals of aircraft at airport  $\alpha$  through time  $t$  by  $\eta_\alpha(t)$ , we can maximize the total number of arrivals by forming the following objective function:  $\mathbf{max} : J = \sum_{\alpha \in \mathbb{A}} \eta_\alpha(T)$ . If we let a link terminating at airport  $\alpha$  be denoted by  $k_\alpha$ , then  $k_\alpha$  belongs to the subset of links terminating at one of

the airports in the set of all airports defined by  $\mathbb{K}_{\mathbb{A}} \subseteq \mathbb{K}$ . We note that the integral  $\int_0^t q_{k_\alpha}(L_{k_\alpha}, s) ds$  represents the cumulative arrivals  $\eta_\alpha(t)$  at airport  $\alpha$  at time  $t$ , and so this objective can be implemented in terms of the flux as

$$\min : J = - \sum_{k_\alpha \in \mathbb{K}_{\mathbb{A}}} \int_0^T q_{k_\alpha}(L_{k_\alpha}, t) dt \quad (7)$$

where  $\mathbf{max} : J = -\mathbf{min} : -J$  has been used to obtain a convex minimization program in standard form. Note that the throughput objective function is linear in the flux function  $q$ . With a proper (linear) discretization in space and time, it will lead to a linear program when subject to linear constraints. This objective function is used in Sections III and IV to highlight the correct numerical implementation of the convex optimization problem.

We introduce a second control objective: to minimize delays by matching the desired flight plans as closely as possible. This is accomplished by first computing the desired density and flux distributions  $\rho_{k, \text{des}}(x, t)$  and  $q_{k, \text{des}}(x, t)$  corresponding to the desired flight plans of all aircraft in the network. In practice, this is a useful formulation when some unforeseen event, such as inclement weather, reduces the capacity of the network and forces deviations from the desired schedule

$$\min : J = \sum_{k \in \mathbb{K}} \int_0^T \int_0^{L_k} \left( (q_k(x_k, t) - q_{k, \text{des}}(x_k, t))^2 + (\rho_k(x_k, t) - \rho_{k, \text{des}}(x_k, t))^2 \right) dx_k dt. \quad (8)$$

This objective will be implemented as a quadratic program when subject to linear constraints and is demonstrated on a benchmark problem implemented in Section V.

To emphasize the usefulness of the convex framework, we note that a third control objective can also be implemented, which is to match a desired arrival schedule at all airports as closely as possible [31]. If we define the desired number of aircraft that have arrived at airport  $\alpha$  by time  $t$  as  $\eta_{\alpha, \text{des}}(t)$ , the objective formulation is  $\mathbf{min} : J = \sum_{\alpha \in \mathbb{A}} \int_0^T (\eta_\alpha(t) - \eta_{\alpha, \text{des}}(t))^2 dt$ . In terms of the flux function, this objective can be written as

$$\min : J = \sum_{k_\alpha \in \mathbb{K}} \int_0^T \left( \int_0^t q_{k_\alpha}(L_{k_\alpha}, s) ds - \int_0^t q_{k_\alpha, \text{des}}(L_{k_\alpha}, s) ds \right)^2 dt. \quad (9)$$

Again, this objective can be implemented as a quadratic program when subjected to linear constraints.

For the objective functions involving scheduling, such as maximizing the throughput of the network (7), a choice of  $T \leq 24$  h is natural. The optimal control strategies can be computed as soon as the flight plans of each aircraft are established for the day. In the event of a perturbation that creates deviations from a prescribed flight plan (8) or arrival schedule (9),  $T$  may range between 6 and 12 h, or a time at which the perturbation no longer effects the flight schedule. Although it is computationally feasible, we do not consider  $T \geq 24$  h simply because other control strategies such as grounding flights become more appropriate. The framework presented in this paper assumes scheduled flights will eventually take place.

### III. PRACTICAL IMPLEMENTATION

#### A. Description of Discretization Schemes

Even though the transformation leading to (6) results into a convex optimization program with linear constraints, which is a significant theoretical improvement with respect to an earlier formulation [4], [40], one still needs to pose (6) in a standard form to be able to solve it numerically. We now explain how the use of linear discretization schemes can lead to LP and QP formulations of (6), thus rendering numerical solutions tractable.

1) *Notation*: For each link in the network, we must discretize the continuous variables into their discrete forms. Dropping the link subscript  $k$  for brevity, the physical domain for  $\rho(x, t)$  and  $q(x, t)$  with  $(x, t) \in [0, L] \times [0, T]$  is written in terms of the discrete variables  $\rho_i^n$  and  $q_i^n$ , where  $i$  and  $n$  are integers in  $[0, i_{\max}]$  and  $[0, n_{\max}]$ , respectively, where  $i_{\max} + 1$  and  $n_{\max} + 1$  correspond to the number of discretization points in space and time. Letting  $\lfloor \cdot \rfloor$  denote the floor operator, we define  $i$  in terms of the continuous space  $x$  and the discrete space step size  $\Delta x$  as  $i = \lfloor x/\Delta x \rfloor$ , and note that  $i_{\max} + 1$  corresponds to the number of discretization points in the space domain. Similarly,  $n$  is defined in terms of the continuous time variable  $t$  and the discrete time step size  $\Delta T$  as  $n = \lfloor t/\Delta T \rfloor$ , and  $n_{\max} + 1$  equals the number of discretization points in time. By applying the discretization, the problem size is reduced from an optimization program with two continuous variables in space and time to a program of size  $= 2(n_{\max} + 1)(i_{\max} + 1)$ .

2) *Explicit and Implicit Schemes*: In general, finite difference schemes can be classified as either implicit or explicit, depending on how the solution of the discrete variables is computed. Explicit finite difference schemes are methods that transform the differential equation into discrete equations in which one computes the unknowns at the current time step using only information known at the previous time step. Starting with a known initial condition at all discrete points in space, the computation of the

unknowns marches forward in time until all unknowns are computed. The advantage of this type of scheme for forward simulation is that there is no need to solve a large system of coupled equations, which can be computationally expensive. In the optimization framework, this type of discretization scheme produces constraints with less coupling, which in turn produces faster run times in practice. The main drawback of using explicit schemes for hyperbolic PDEs (such as the modified LWR PDE), is that they are conditionally stable at best [37], as first proved in [11]. The stability condition imposes a constraint between the size of the discrete time step and the discrete space step. In practice, this often leads to unnecessarily large number of time steps (due to a required small discretization in time) to achieve a desired level of accuracy in the space domain.

One way of overcoming this restriction is to use of unconditionally stable implicit finite difference schemes. In forward simulation, the discrete variables at each time step are computed using unknown variables at both the past and future time steps. As a result, the discrete system of equations must be solved simultaneously. In the optimization framework, this imposes no additional complexity in formulating the problem; however, it results in more highly coupled constraints, which may increase the computational time for a solver to find the solution to the corresponding problem.

3) *Schemes Implemented*: We now describe the difference equations obtained by applying a variety of finite difference schemes to the modified LWR PDE constraint (6).

- The (explicit) *Lax–Friedrichs* (LxF) scheme is written in terms of  $\rho(x, t)$  and  $q(x, t)$  as [15]

$$\rho_i^{n+1} = \frac{1}{2}(\rho_{i+1}^n + \rho_{i-1}^n) - \frac{1}{2} \frac{\Delta T}{\Delta x} (q_{i+1}^n - q_{i-1}^n) \quad (10)$$

which is subject to the *Courant–Friedrichs–Lewy* (CFL) condition:  $|(\Delta T/\Delta x)v_i^n| \leq 1$  for stability [15]. Since  $v_i^n$  is an unknown optimization variable, we must ensure stability for all possible  $v_i^n$ , namely,  $|(\Delta T/\Delta x)v_{\max}| \leq 1$ .

- The (implicit) *first-order forward difference in time, second-order centered difference in space* (2CD) scheme is written as

$$\rho_i^{n+1} = \rho_i^n - \frac{1}{2} \frac{\Delta T}{\Delta x} (q_{i+1}^{n+1} - q_{i-1}^{n+1}). \quad (11)$$

- The (implicit) *first-order forward difference in time, fourth-order centered difference in space* (4CD) scheme is written as

$$\rho_i^{n+1} = \rho_i^n - \frac{1}{12} \frac{\Delta T}{\Delta x} (-q_{i+2}^{n+1} + 8q_{i+1}^{n+1} - 8q_{i-1}^{n+1} + q_{i-2}^{n+1}). \quad (12)$$

- Alternatively, if the second-order centered difference in space at the  $t$  and  $t + 1$  time steps are averaged, the (implicit) *Crank–Nicholson* (CN) scheme is obtained [37]

$$\rho_i^{n+1} = \rho_i^n - \frac{\Delta T}{4\Delta x} (q_{i+1}^{n+1} - q_{i-1}^{n+1} + q_{i+1}^n - q_{i-1}^n). \quad (13)$$

- The (implicit) *first-order forward difference in time, first-order upwind in space* (1UP) is written as [15]

$$\rho_i^{n+1} = \rho_i^n - \frac{\Delta T}{\Delta x} (q_i^{n+1} - q_{i-1}^{n+1}). \quad (14)$$

- The (implicit) *first-order forward difference in time, second-order upwind in space* (2UP) is written as [15]

$$\rho_i^{n+1} = \rho_i^n - \frac{1}{2} \frac{\Delta T}{\Delta x} (3q_i^{n+1} - 4q_{i-1}^{n+1} + q_{i-2}^{n+1}). \quad (15)$$

Additionally, a variety of modifications can be made to the LxF, 2CD, 4CD, and CN schemes to introduce asymmetry in the schemes, which we now present. This prevents undesirable “sawtooth-like” oscillations in the solutions of the optimization problems presented in the next section.

- The (implicit) *modified second-order centered difference* (M2CD) scheme is written as

$$\rho_i^{n+1} = \rho_i^n - \frac{1}{2} \frac{\Delta T}{\Delta x} \left( \frac{1}{2} (q_{i+2}^{n+1} + q_i^{n+1}) - q_{i-1}^{n+1} \right). \quad (16)$$

- The (implicit) *modified fourth-order centered difference* (M4CD) scheme is written as

$$\rho_i^{n+1} = \rho_i^n - \frac{1}{12} \frac{\Delta T}{\Delta x} \left( -q_{i+2}^{n+1} + \frac{1}{2} (8q_{i+2}^{n+1} + 8q_i^{n+1}) - 8q_{i-1}^{n+1} + q_{i-2}^{n+1} \right). \quad (17)$$

- The 1UP inspired (implicit) *modified Crank–Nicholson* (MCN) scheme is written as

$$\rho_i^{n+1} = \rho_i^n - \frac{\Delta T}{2\Delta x} (q_i^{n+1} - q_{i-1}^{n+1} + q_i^n - q_{i-1}^n). \quad (18)$$

- Finally, we also test the (implicit) *Crank–Nicholson with dissipation* (CND) scheme [15]

$$\rho_i^{n+1} = \rho_i^n - \frac{\Delta T}{4\Delta x} (q_{i+1}^{n+1} - q_{i-1}^{n+1} + q_{i+1}^n - q_{i-1}^n) - \frac{\varepsilon}{16} (q_{i+2}^n - 4q_{i+1}^n + 6q_i^n - 4q_{i-1}^n + q_{i-2}^n) \quad (19)$$

which has a dissipative term of order 4 for small values of  $\varepsilon$  (i.e.,  $\varepsilon = (1/2)$ ).

Schemes (16)–(18) are developed by introducing an asymmetric term in  $q$ , which is simply an average of the two neighboring points. For example, in (11), point  $q_{i+1}^{n+1}$  is replaced with its approximation  $(1/2)(q_{i+2}^{n+1} + q_i^{n+1})$ . This slight asymmetry can significantly reduce the likelihood of nonphysical “sawtooth-like” oscillations, which are described in detail in Section IV-A.

4) *Boundary Conditions*: When implementing any numerical scheme, special attention must be paid to boundary conditions. In this optimization program, we implement the boundary conditions in the strong sense at the first grid point in the physical domain because it is an inflow condition. Downstream, we implement boundary conditions with ghost points, following the procedure outlined in [38] and [40]. This is now presented on the LxF scheme, while noting that a similar procedure is used on the other schemes.

The initial distribution of density on each link  $k$ , given by  $\rho_{t_0,k}(x)$ , is directly imposed in the discrete problem as follows:

$$\rho_{i,k}^0 = \rho_{t_0,k}(i\Delta x). \quad (20)$$

If the initial velocity profile  $v_0(x)$  at the initial time is also known, the initial flux profile can be defined similarly as

$$q_{i,k}^0 = \rho_{t_0,k}(i\Delta x)v_0(i\Delta x). \quad (21)$$

At the link entrance, we impose the inflow flux on link  $k$  on the discrete flux variable  $q_{0,k}^n$  according to

$$q_{0,k}^n = q_{x_0,k}(n\Delta T) + \sum_{m \in \mathbb{M}_k} \beta_{m,k} q_m(i_{\max}\Delta x, n\Delta T). \quad (22)$$

This expression can be interpreted as follows. The discrete flux variables  $q_{0,k}^n$  on each link  $k$ , at the boundary  $i = 0$ , is equal to the inflow flux function  $q_{x_0,k}(t)$  representing all aircraft entering the network at link  $k$ , plus the fluxes from all links that feed flow already in the network into link  $k$ . The density along the link entrance  $\rho_{0,k}^n$  is bounded but not specified directly at this boundary; its optimal value is computed directly from the optimization program.

With variables now defined along the initial time and space boundaries, the LxF scheme (10) is encoded as a constraint involving  $\rho_i^n$ ,  $\rho_{i+1}^n$ ,  $\rho_{i-1}^n$ ,  $q_{i+1}^n$ , and  $q_{i-1}^n$  for all  $i \in [1, i_{\max}]$  and  $n \in [1, n_{\max}]$ . Because  $\rho_{i+1}^n$  and  $q_{i+1}^n$  are undefined in the PDE evaluation at  $i_{\max}$ , we introduce a ghost point at  $i_{\max} + 1$  that is not in the physical domain. Instead, it is used for the sole purpose of computing the flux and density variables at the link exit according to the discretized PDE constraint. These variables are constrained to the physical system by invoking the constraints

$$\rho_{i_{\max}+1}^n = \rho_{i_{\max}}^n, \quad q_{i_{\max}+1}^n = q_{i_{\max}}^n. \quad (23)$$

Note that for higher order schemes, such as 4CD, it is necessary to add an additional ghost point at the downstream point  $i = i_{\max} + 2$  as well as at the upstream point  $i = -1$ .

## B. Computational Results

We now discuss the accuracy and computation time of the numerical schemes. We solve the following maximization of throughput *validation problem* on a single link

$$\begin{aligned} \min : & \quad - \int_0^T q(L, t) dt \\ \text{st} : & \quad \frac{\partial \rho(x, t)}{\partial t} + \frac{\partial q(x, t)}{\partial x} = 0 \\ & \quad q(0, t) = q_{x_0}(t) \\ & \quad \rho(x, 0) = \rho_{t_0}(x) \\ & \quad -\frac{1}{5} \leq \rho(x, t) \leq 3 \\ & \quad \rho(x, t)v_{\min}(x, t) \leq q(x, t) \\ & \quad \leq \rho(x, t)v_{\max}(x, t) \end{aligned} \quad (24)$$

where  $q_{x_0}(t)$  is a bump inflow condition

$$q_{x_0}(t) = \begin{cases} 0 & \text{for } t \leq \frac{1}{4} \\ \sin(2\pi(1-2t)) & \text{for } t \in [\frac{1}{4}, \frac{1}{2}] \\ 0 & \text{for } t \geq \frac{1}{2} \end{cases} \quad (25)$$

$\rho_{t_0}(x)$  is the initial density distribution

$$\rho_{t_0}(x) = \begin{cases} \sin(2\pi x) & \text{for } x \in [0, \frac{1}{2}] \\ 0 & \text{for } x \in [\frac{1}{2}, 2] \end{cases} \quad (26)$$

and the velocity bounds  $v_{\max}(x, t)$  and  $v_{\min}(x, t)$  are equal

$$\begin{aligned} v_{\max}(x, t) &= v_{\min}(x, t) \\ &= \begin{cases} 2 & \text{for } x \in [0, 1], \forall t \\ 3-x & \text{for } x \in [1, 2], \forall t. \end{cases} \end{aligned} \quad (27)$$

As can be seen by inspection, the feasible set of program (24) is reduced to a single point in the  $(\rho(\cdot, \cdot), q(\cdot, \cdot))$  space, defined by the constraint  $q(x, t) = v_{\min}(x, t)\rho(x, t) = v_{\max}(x, t)\rho(x, t)$  and the initial and boundary conditions, which make the problem well posed, and the solution subsequently unique.

Solving (24) as an optimization program (rather than as a forward simulation of the numerical scheme) provides experimental evidence that the numerical solver used works properly, when checked against the easily computed analytical solution of the problem.

For this problem, the upper bound constraint on the density equal to three is not an active constraint. The lower bound has been relaxed to  $-(1/5)$  to allow for overshoot errors introduced by the discretization. Note that the upper and lower bounds for the velocity are a function of time and space and are equal and piecewise continuous. This same velocity profile can be used to compute the exact solution to the PDE according to the solution obtained by the method of characteristics [4]. Thus, we can compare the accuracy of the optimal solution of the finite difference equation with the exact analytic solution.

Next, we relax the constraint that  $v_{\min}(x, t) = v_{\max}(x, t)$  and examine the solve time for the *control problem*. The velocity profile for the control problem is given as

$$\begin{aligned} v_{\max}(x, t) &= 2 \\ v_{\min}(x, t) &= \begin{cases} 2 & \text{for } x \in [0, 1], \forall t \\ 3-x & \text{for } x \in [1, 2], \forall t \end{cases} \end{aligned} \quad (28)$$

where the lower bound on the velocity has been relaxed. Note that the space  $v_{\min}(x, t)\rho(x, t) \leq q(x, t) \leq v_{\max}(x, t)\rho(x, t)$  is not reduced to a single point, leaving room for control, as solved by substituting (28) into (24).

In order to compare the various discretization schemes (10)–(19), the error  $\rho_e$  of the discrete density field is computed using the Frobenius norm [25]

$$\rho_e := \frac{1}{n_{\max} i_{\max}} \sum_{n=0}^{n_{\max}} \sum_{i=0}^{i_{\max}} |\rho_i^n - \rho(i\Delta x, n\Delta T)|^2$$

where the additional  $1/n_{\max} i_{\max}$  term is added to standardize the error computation across different levels of discretization. The error computed here is the error

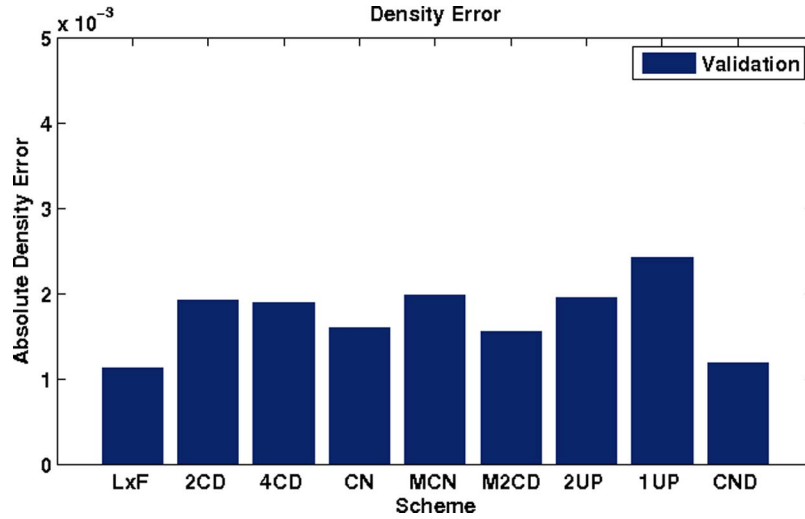


**Fig. 2.** Comparison of errors (vertical axis) between the optimal solution for density to validation problem (24) computed by each scheme (horizontal axis) and the exact solution. The computations are performed with 60 points in space  $x \in [0, 2]$ , 120 points in time  $t \in [0, 2]$ , 7200 discrete density optimization variables.

introduced by the discretization of the continuous form of the PDE model. The error between the PDE model and the individual aircraft trajectories is addressed in [40], where it is found to be the most accurate of the four aggregate models compared in that work. The results displayed in Fig. 2 indicate that the LxF and the CND scheme have the highest accuracy, with an absolute density error on the order of 0.001 per discrete point  $\rho_i^n$ .

We compare the computation time of the respective schemes in Fig. 3. The cost of the explicit schemes prevents them from being practical for large networks, with the exception of 1UP and the MCN scheme inspired

by the 1UP scheme. Additionally, the 2UP and CND schemes cannot be used to solve the control problem, since they result in infeasible programs, described subsequently. In terms of speed, the LxF scheme outperforms the implicit schemes, due to its explicit structure.

The results from this benchmark scenario demonstrate results typical of this type of optimization.

#### IV. IMPLEMENTATION ISSUES

One of the contributions of this paper is the proper selection and use of appropriate numerical schemes to

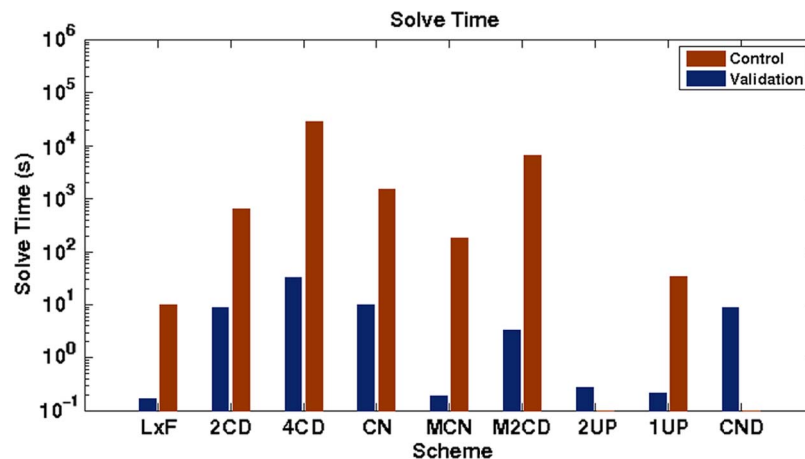


**Fig. 3.** Comparison of the computational time (vertical axis) required by each of the different schemes (horizontal axis) to solve the validation problem (24) (blue) and the its corresponding control problem (28) (red). The computation is realized with 60 points in space  $x \in [0, 2]$ , 120 points in time  $t \in [0, 2]$ , 14 400 optimization variables.

pose the continuous convex optimization problem in a discrete form. As revealed by the work described in this paper, while (6) or its discrete counterpart is convex in theory, a simple implementation of these programs that does not take into account specific features of the numerical schemes often results in (numerical) infeasibility or meaningless solutions. This occurs even when physically meaningful solutions exist for the continuous programs.

To illustrate the implementation challenges, the optimization program (24) is discretized for one link. We show the full problem discretization with the LxF scheme and note that a similar procedure is followed for other schemes. The discretization results in the following problem:

$$\begin{aligned}
 \min : & \quad - \sum_{n=0}^{n_{\max}} q_{i_{\max}}^n \Delta T \\
 \text{st} : & \quad \rho_i^{n+1} = \frac{1}{2}(\rho_{i+1}^n + \rho_{i-1}^n) - \frac{1}{2} \frac{\Delta T}{\Delta x} (q_{i+1}^n - q_{i-1}^n), \\
 & \quad \quad \quad i \in [1, i_{\max}], n \in [1, n_{\max}] \\
 & \quad \rho_{i_{\max}}^{n+1} = \frac{1}{2}(\rho_{i_{\max}}^n + \rho_{i_{\max}-1}^n) \\
 & \quad \quad - \frac{1}{2} \frac{\Delta T}{\Delta x} (q_{i_{\max}}^n - q_{i_{\max}-1}^n), \quad n \in [1, n_{\max}] \\
 & \quad q_0^n = q_{x_0}(n\Delta T), \quad n \in [1, n_{\max}] \\
 & \quad \rho_i^0 = \rho_{t_0}(i\Delta x) \quad i \in [1, n_{\max}] \\
 & \quad -\frac{1}{5} \leq \rho_i^n \leq 3, \quad i \in [1, i_{\max}], \quad n \in [1, n_{\max}] \\
 & \quad \rho_i^n v_{i,\min}^n \leq q_i^n \leq \rho_i^n v_{i,\max}^n \\
 & \quad \quad \quad i \in [1, i_{\max}], n \in [1, n_{\max}] \quad (29)
 \end{aligned}$$

where the second constraint represents the discretized PDE with the ghost points correctly implemented at the

link exit boundary. The inflow constraint  $q_{x_0}(t)$  is given by (25),  $\rho_{t_0}(x)$  is given by (26), and the velocity bounds are given by

$$\begin{aligned}
 v_{i,\max}^n &= v_{i,\min}^n \\
 &= \begin{cases} 2 & \text{for } i\Delta x \in [0, 1] \\ 3 - x & \text{for } i\Delta x \in [1, 2]. \end{cases} \quad (30)
 \end{aligned}$$

### A. Infeasibility

One ironic feature of the numerical implementation is the fact that a problem can become infeasible by relaxing the velocity constraint from  $v_{\min}(x, t) = v_{\max}(x, t)$  to  $v_{\min}(x, t) < v_{\max}(x, t)$ : apparently increasing the feasible set results in infeasibility. This is the case for the 2UP and CND schemes. To see why this occurs, we examine the second constraint in (6):  $v_{\min}(x, t)\rho(x, t) \leq q(x, t) \leq v_{\max}(x, t)\rho(x, t)$ . In the framework of air traffic control, the density and flux should remain nonnegative to be physically meaningful. However, the discrete formulations of the LWR PDE can introduce an overshoot, which causes the density to become slightly negative (see Fig. 4). In the problem formulation, we can relax the explicit constraint that  $\rho(x, t) \geq \rho_{\min} = 0$  to accommodate this numerical error. In the validation problem, this causes a proportional negative flux, but the problem remains feasible (assuming it does not violate the relaxed  $\rho_{\min}$  constraint). The same cannot be said for the control problem. Even when the  $\rho_{\min}$  constraint is relaxed to allow for overshoot, the problem formulation has an implicit constraint that  $\rho(x, t) \geq 0$ . To see why, we assume  $\rho(x, t) \leq 0$  and note that the constraint on  $q$  would become

$$\begin{aligned}
 v_{\min}(x, t) \cdot (-1)|\rho(x, t)| &\leq q(x, t) \\
 &\leq v_{\max}(x, t) \cdot (-1)|\rho(x, t)| \quad (31)
 \end{aligned}$$

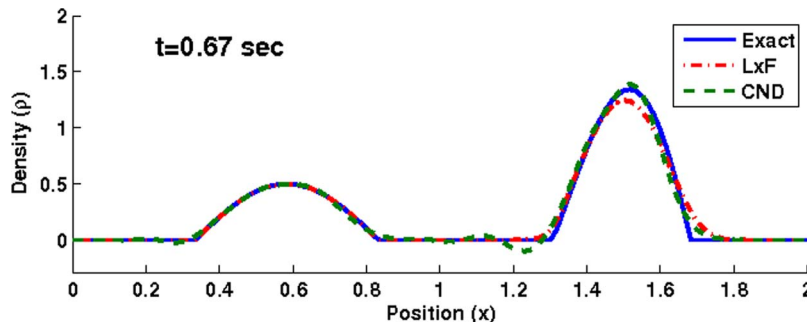


**Fig. 4.** Comparison of the computed density LxF (dash-dot red) and CND (dashed green) schemes and the exact solution (solid blue) to (24) at time  $t = 0.67$  s. Vertical axis: density ( $\rho$ ). Horizontal axis: position ( $x$ ). The LxF scheme is feasible for the control problem, while the CND scheme is infeasible because of the undershoot clearly visible, which violates  $\rho(x, t) \geq 0$  locally due to numerical inaccuracy.

which leads to the following contradiction:

$$v_{\min}(x, t) \geq v_{\max}(x, t). \quad (32)$$

Thus, schemes such as CND, which are very accurate overall for the validation problem, cannot be used for the control problem because of a slight negative overshoot (see Fig. 4), making the optimization program infeasible.

### B. Physically Meaningless Solutions

Another implementation challenge occurs when implicit schemes such as 2CD, 4CD, and CN are used in the optimization framework of (6). Although these schemes are unconditionally stable, they may still suffer from significant oscillations, as shown in Fig. 5. This figure shows the result of solving a control problem with constant initial and boundary conditions. The observed oscillations are a direct consequence of the symmetric centered spatial difference of  $\partial q(x, t)/\partial x$  that appears each of these schemes [(11)–(13)]. This symmetry opens the potential for solutions to the discretized PDE that are not solutions to its continuous counterpart. For example, consider the original PDE constraint  $(\partial \rho(x, t)/\partial t) + (\partial q(x, t)/\partial x) = 0$  and impose an additional constraint that  $(\partial \rho(x, t)/\partial t) = 0$  for all  $x$  and all  $t$ . In the continuous framework, any solution to the optimization problem with this constraint must necessarily satisfy  $(\partial q(x, t)/\partial x) = 0$ . Taking the discrete version of this condition by applying a centered difference operator on the spatial derivative of  $q$ , we find there are multiple solutions to the discretized constraint  $(q_{i+1}^n -$

$q_{i-1}^n/2\Delta x) = 0$ . One such solution, corresponding to the analytic solution of the continuous constraint, is

$$q_0^n = q_1^n = \dots = q_{i_{\max}}^n = C \quad (33)$$

where  $C$  is a constant. A more pathological solution to the difference equation can be expressed as

$$\begin{aligned} q_1^n &= q_3^n = q_5^n = \dots = C_1 \\ q_0^n &= q_2^n = q_4^n = \dots = C_2 \end{aligned} \quad (34)$$

where  $C_1$  and  $C_2$  are constants. Here, the spatial profile of the flux oscillates between the values of  $C_1$  and  $C_2$ , and therefore would not satisfy the continuous constraint in the limit:  $\partial q/\partial x = 0$ . On the other hand, it does satisfy the discrete constraints

$$\begin{aligned} \left(\frac{\partial q}{\partial x}\right)_{i=2} &= \frac{q_3 - q_1}{2\Delta x} = \frac{C_1 - C_1}{2\Delta x} = 0 \\ \left(\frac{\partial q}{\partial x}\right)_{i=3} &= \frac{q_4 - q_2}{2\Delta x} = \frac{C_2 - C_2}{2\Delta x} = 0. \end{aligned} \quad (35)$$

Thus, this solution exists only in the discrete representation of the problem and does not correspond to the physics of air traffic flows on the network.

Clearly, discrete models using the central difference operator have a potential for solutions with large deviations from the continuous model because they allow

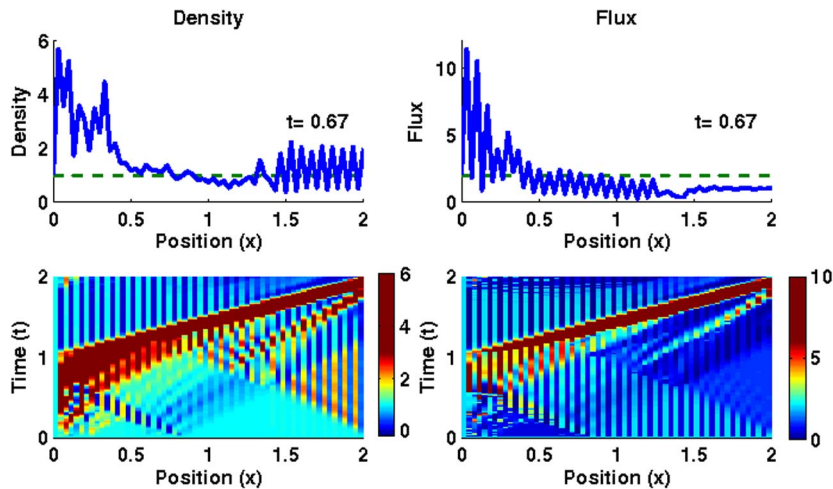


**Fig. 5.** Density (left column) and flux (right column) solutions to a control problem with constant boundary and initial conditions:  $q(0, t) = 2$ ,  $\rho(x, 0) = 1$ , with  $v_{\min} = 0.5$  and  $v_{\max} = 2$ , at time  $t = 0.67$  (top row). Surface plots of the density and flux (bottom row) show the solution exhibits oscillatory behavior.

too much freedom for the solution to oscillate. One way to prevent this phenomenon is to use an asymmetric scheme to compute the space derivatives, similar to those used for the temporal derivatives. For example, if we examine the first-order upwind scheme approximation for the spatial derivatives on  $q$

$$\left(\frac{\partial q}{\partial x}\right) = \frac{q_{i+1}^n - q_i^n}{\Delta x} \quad (36)$$

we see that no oscillations are possible. If  $\partial q/\partial x = 0$ , the unique solution, its discrete representation is  $q_{i+1} = q_i = C$  for all  $i$ . Thus, the potential for oscillatory solutions for stable discretization step-sizes can be greatly reduced by adding an asymmetric term in the finite difference scheme, as was done in (16)–(18). The pathological cases presented in this section unfortunately happen frequently in practice due to the nature of algorithms running in optimization software such as CPLEX.

The proper selection of a good numerical scheme, as presented earlier, avoids the two pitfalls presented in Section IV-A and B, which are not obvious when “blindly” implementing the convex program (24).

## V. APPLICATION TO THE OAKLAND AIR ROUTE TRAFFIC CONTROL CENTER

### A. Model Construction

Using previous modeling work (see [39] and [40]), we now apply the proposed algorithm to the en route and arrival airspace in the Oakland Center, which we have studied in the past and for which we have a database of data from the *Enhanced Traffic Management System* (ETMS) and

*Aircraft Situation Display to Industry* (ASDI). In [40], we have validated a model of en route traffic flow against this data and assessed its accuracy. We use a subset of links from this model, which is relevant for our application. The selected network, depicted in Fig. 6, consists of 14 links merging into the Oakland Terminal Radar Approach Control (TRACON), in which traffic follows a fifteenth link. Following the procedure outlined in [39], the link network is generated by aggregating all air traffic data from October 1, 2004, to September 30, 2005. Corresponding historical velocity profiles  $v(x)$  can be identified from the database. In the case presented in the earlier section, the profiles result from the optimization algorithm and depend on time (speed control policies). However, as was presented in Section III, by nature of the optimization, a range of feasible velocity profiles is prescribed to the algorithm (from which a globally optimal profile is captured). We construct this range from the historical mean, from which we allow speed amendments of  $\pm 15\%$ .

### B. Flow Simulation

In the simulation presented next, aircraft enter the network at the boundaries of 9 different links shown in Fig. 6 (right). During the first four hours of the six-hour simulation, 117 aircraft enter the network. We convert each entering aircraft into a flux  $q$  used in the LWR PDE. Assuming the  $i$ th aircraft enters link  $k$  at time  $t_i^k$ , it generates a flux  $q_{x_0,k,i}(t)$  on the link over a time window  $z$ , according to the following:

$$q_{x_0,k,i}(t) = \begin{cases} \sin\left(\frac{t - (t_i^k - \frac{z}{2})}{z} \pi\right) & t \in [t_i^k - \frac{z}{2}, t_i^k + \frac{z}{2}] \\ 0 & \text{otherwise.} \end{cases} \quad (37)$$

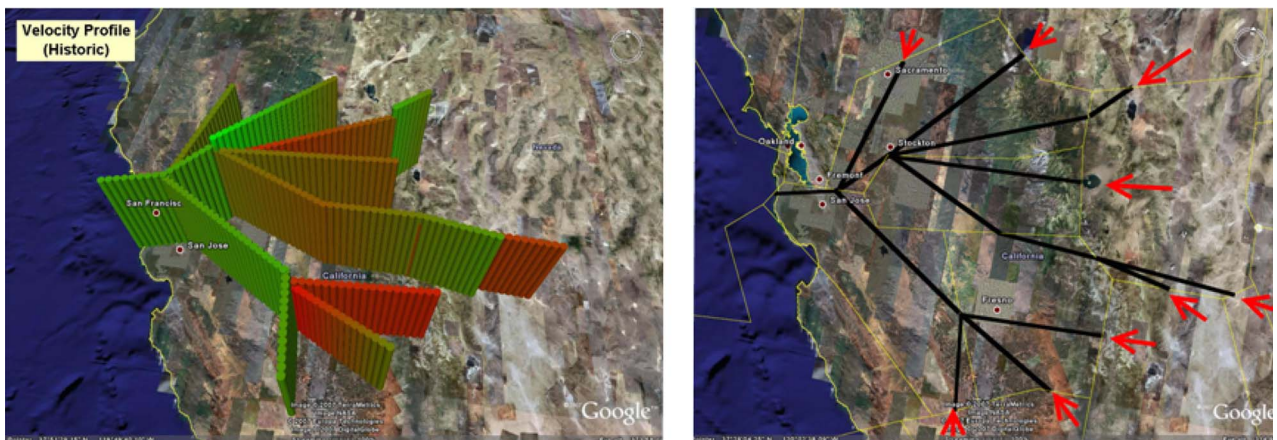


**Fig. 6.** (Left) Aggregate velocity profiles for each of the 15 links generated from actual flights on January 1, 2005, with increasing height corresponding to increasing velocity. The leftmost link corresponds to the Oakland TRACON entrance. (Right) Links with incoming inflows are denoted with arrows.

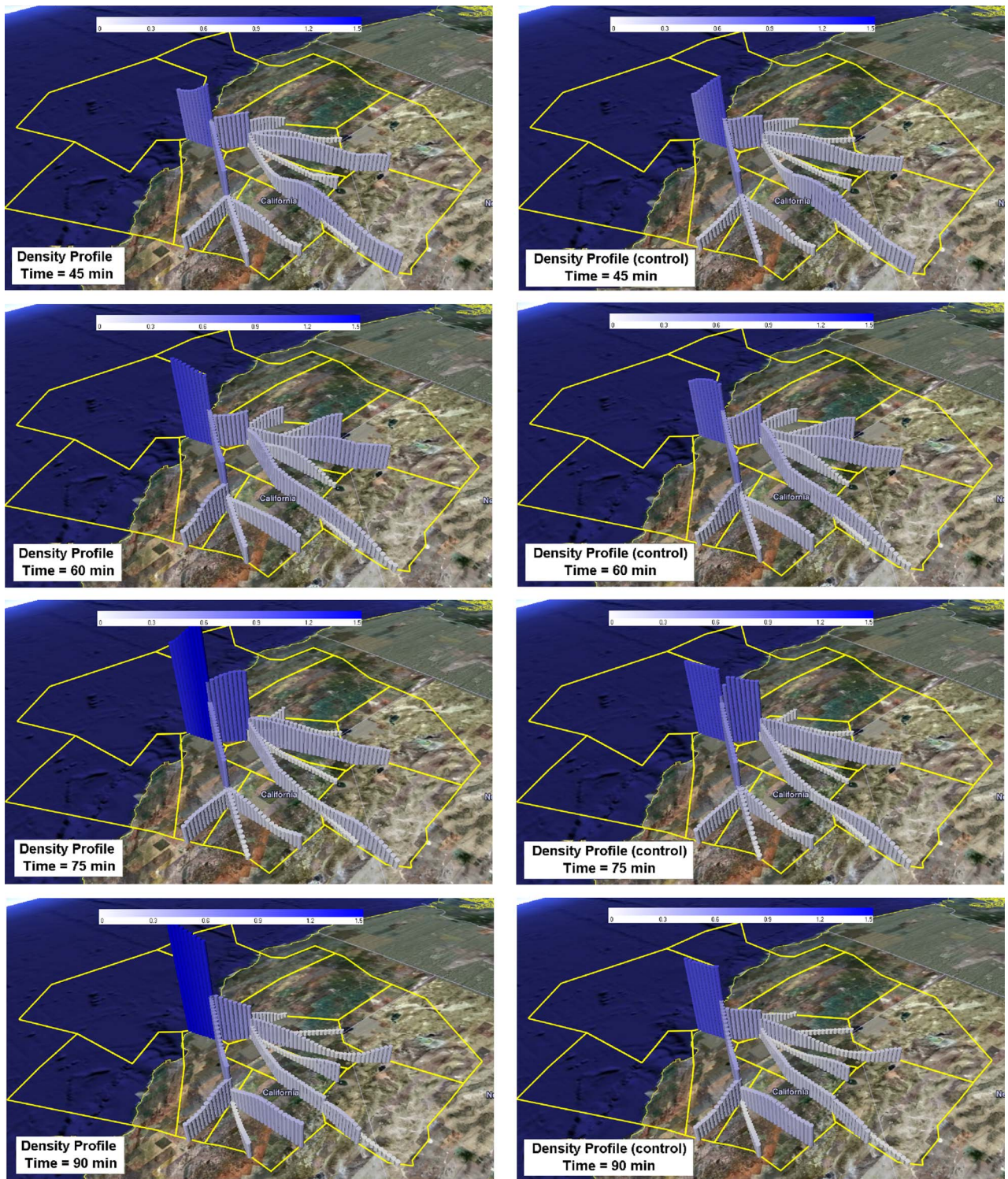


**Fig. 7.** Results showing the evolution of density on the network operating at (left) full capacity and (right) 66% full capacity from (top) time 45 minutes, increasing in 15 minute increments to (bottom) time 90 minutes. Increasing height and darkening color indicates the increasing density on the links.

The link flux boundary condition  $q_{x_0,k}(t)$  is then obtained by summing the flux contributions over all aircraft entering the link  $q_{x_0,k}(t) = \sum_i q_{x_0,k,i}(t)$ . This form

of aggregation is easy to implement and can be tracked easily in the forward simulation. With velocity profiles obtained from the flights on January 1, 2005 [Fig. 6 (left)]

and the inflow boundary conditions given by (6), we run the forward simulation to check the validity of the model. The computations are performed with the LxF scheme, assuming a discrete spatial step of 4 nautical miles and a discrete time step of 31 s, corresponding to a maximum CFL condition number of 0.7801. This optimization program has 357 072 variables, and the solution is computed in 4 s on a standard laptop running CPLEX (which uses an interior point algorithm). Note that a feasible solution to this program is equivalent to a forward simulation of the problem. The corresponding results are illustrated in Fig. 7. These figures show a sharp density increase at the edges of the links nearest to the Oakland TRACON, which is a direct result of the bottleneck geometry of the network and merging traffic. The density of aircraft peaks at seven aircraft on the last link, which is 33 nautical miles long.

### C. Network Optimization Under Reduced Capacity

We now consider a scenario in which the capacity of each link in the network reduced to 66% of the capacity under the nominal conditions. This decrease in capacity may have several causes—for example, outgoing traffic, special use airspace, and weather disturbances. Although the capacity on a given portion of the network may be reduced, our objective is to minimize the effect of this capacity decrease on traffic through the network. In other words, we wish to find the optimal velocity control strategies for each link in the network that satisfies the reduced capacity constraint, using the smallest speed amendments possible. This objective is formally stated as (8), where  $q_{k,des}^n$  and  $\rho_{k,des}^n$  are the flux and density obtained from the unconstrained forward simulation.

In order to meet the reduced capacity constraint, we allow the velocity profiles to increase or decrease by at most 15% from the historical average on each link. We use the same discretization scheme as the forward simulation and verify that the CFL condition still holds for a 15% increase in the maximum velocity. The quadratic optimization problem runs in 45 s on average, outperforming adjoint-based methods [40] by at least one order of magnitude for speed of computation, with the added benefit of providing a globally optimal solution to the problem. Thus, for a given set of inflows into the network, a forward simulation and optimization to find a solution meeting a reduced capacity constraint can be completed in less than a minute on a standard laptop for the entire arrival airspace shown in the right column of Fig. 6. The globally optimal changes to the density evolution caused by a 33% reduction in the capacity are displayed in the right column of Fig. 7, in which the height on each link corresponds to the magnitude of the density. In the left column, the aircraft flow evolves according to the mean historic velocity computed for each link. As the aircraft converge towards the Oakland TRACON, the density of aircraft increases significantly relative to other parts of the

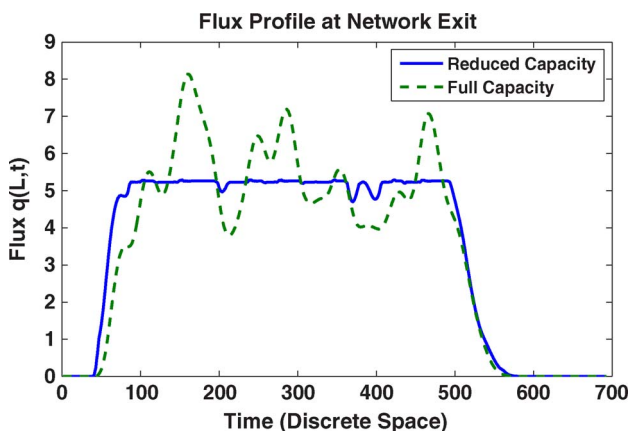


Fig. 8. Comparison of the flux profile (vertical axis) at the last point in the network, for the unconstrained (dotted) network and the network with 66% reduced capacity (solid).

network. In the right column, the aircraft evolve according to the globally optimal velocity control. We observe that the reduced capacity density constraint is active on the link into Oakland for time  $t = 75$  min and at  $t = 90$  min, which means the link is operating at 100% of the reduced capacity. Because of the certificate of global optimality, and because the resulting objective is positive definite [9], this is the unique globally optimal solution that minimizes changes to the flight schedule.

The striking feature of the reduced capacity simulations is that minimal changes to the aircraft density upstream can lead to significant changes in the link downstream. Furthermore, we can examine the schedule of aircraft exiting the network under full and reduced capacity in Fig. 8. The peaks in the full capacity simulation correspond to times when a large number of aircraft is arriving simultaneously into the Oakland TRACON. The valleys show periods when fewer aircraft are arriving into the TRACON. As a result of the reduced capacity, the desired arrival schedules of all aircraft cannot be met at the peak time. Instead, the aircraft arrival times must be more evenly distributed in time, as shown in Fig. 8. The benefit of the optimization framework developed in this paper is that the changes to the flight plans are the global minimum that satisfy the reduced capacity constraints.

## VI. CONCLUSION

This paper follows a series of papers on aggregate flow models of air traffic that have been used by NASA as frameworks to study the imbalance between demand and capacity in the National Airspace System. The fundamental contribution of this paper is the formulation of a classical partial differential equation-based optimal control problem (maximization of throughput in a network or

minimization of delays) as a convex program (either quadratic or linear in the present case). This is a significant improvement over previous techniques based on adjoint optimization, which are computationally more demanding and do not provide guarantees of optimality. The formulation proposed here relies on a reformulation of the partial differential equation (nonlinear in the decision variables) as a partial differential equation, which linearly relates derivatives of decision variables after a variable change. The subsequent contribution of this paper is the development of several linear discretization schemes that transform the constraints of the problem into linear constraints, essential to the success of the method. The computational efficiency of the method is studied and shows a decrease if computational time compared to the previous methods by at least one order of magnitude (the solution is computed in seconds on a standard laptop). While convex optimization (and corresponding solvers such as CPLEX) enabled a significant improvement in computational time, this paper also displayed two nontrivial pitfalls underlining the fact that “posing a problem as a convex optimization program” does not provide a systematic solution to engineering problems. In particular, the extensive numerical tests we have made on the nine numerical schemes presented here show that without an appropriate choice of numerical scheme for the problem formulation, the problem may become infeasible

or result in physically meaningless solutions. Even if the schemes are very accurate, overshoots or undershoots can systematically make optimization programs infeasible if some of the constraints are active where the overshoot occurs. Other schemes result in optimal “sawtooth-like” solutions that satisfy all of the constraints yet are physically meaningless. On a practical side, the implementation of the methods proposed in this paper greatly improves upon previous computational results on a benchmark problem presented in the previous section of this paper for the specific case of the Oakland en route airspace. Recent studies in automation of highway transport systems have shown that these techniques (for almost identical partial differential equations) make our results directly applicable to highway traffic flow optimization, which constitutes an interesting outgrowth of this paper that we intend to pursue in the future. ■

### Acknowledgment

The authors are grateful to Dr. R. Raffard for sharing with us his assessment of the feasibility of posing the first problem outlined in this article as a convex program, based on an earlier conversation with Prof. C. Tomlin, A. Jameson, and S. Boyd. They want to thank D. Sun for his help with ETMS/ASDI data and for sharing his numerical database for this project.

### REFERENCES

- [1] S. Amin, A. Bayen, L. El Ghaoui, and S. Sastry, “Robust feasibility for control of water flow in a reservoir-canal system,” in *Proc. 46th IEEE Conf. Decision Contr. Conf.*, New Orleans, LA, Dec. 2007, pp. 1571–1577.
- [2] G. Bastin and V. Guffen, “Congestion control in compartmental network systems,” *Syst. Contr. Lett.*, vol. 55, no. 8, pp. 689–696, 2006.
- [3] A. Bayen, P. Grieder, G. Meyer, and C. Tomlin, “Lagrangian delay predictive model for sector-based air traffic flow,” *AIAA J. Guidance, Contr., Dyn.*, vol. 28, no. 5, pp. 1015–1026, 2005.
- [4] A. Bayen, R. Raffard, and C. Tomlin, “Adjoint-based control of a new Eulerian network model of air traffic flow,” *IEEE Trans. Contr. Syst. Technol.*, vol. 14, no. 5, pp. 804–818, 2006.
- [5] A. Bennett, *Inverse Methods in Physical Oceanography*. Cambridge, U.K.: Cambridge Univ. Press, 1992.
- [6] D. Bertsimas and S. S. Patterson, “The air traffic flow management problem with enroute capacities,” *Oper. Res.*, vol. 46, no. 3, pp. 406–422, 1998.
- [7] K. Bilimoria, B. Sridhar, G. Chatterji, K. Sheth, and S. Grabbe, “FACET: Future ATM concepts evaluation tool,” in *Proc. 3rd USA/Eur. ATM 2001 R&D Seminar*, Naples, Italy, Jun. 2001.
- [8] F. Borrelli, *Constrained Optimal Control of Linear & Hybrid Systems*, vol. 290, *Lecture Notes in Control and Information Sciences*. Berlin, Germany: Springer-Verlag, 2003.
- [9] S. Boyd and L. Vandenberghe, *Convex Optimization*. Cambridge, U.K.: Cambridge Univ. Press, 2004.
- [10] J. Coron, B. d’Andréa-Novel, and G. Bastin, “A strict Lyapunov function for boundary control of hyperbolic systems of conservation laws,” *IEEE Trans. Autom. Control*, vol. 52, no. 1, pp. 2–11, 2007.
- [11] R. Courant, K. Friedrichs, and H. Lewy, “Über die partiellen Differenzgleichungen der mathematischen Physik,” *Math. Ann.*, vol. 100, pp. 32–74, 1928.
- [12] C. Daganzo, “The cell transmission model: A dynamic representation of highway traffic consistent with the hydrodynamic theory,” *Transp. Res. B*, vol. 28, no. 4, pp. 269–287, 1994.
- [13] C. Daganzo, “The cell transmission model, Part II: Network traffic,” *Transp. Res. B*, vol. 29, no. 2, pp. 79–93, 1995.
- [14] Federal Aviation Administration, *FAA Aerospace Forecasts: Fiscal Years 2007–2020*, 2007.
- [15] C. Hirsch, *Numerical Computation of Internal & External Flows: Fundamentals of Numerical Discretization*. New York: Wiley, 1988.
- [16] A. Jameson, L. Martinelli, and N. Pierce, “Optimum aerodynamic design using the Navier-Stokes equations,” *Theor. Comput. Fluid Dyn.*, vol. 10, no. 1, pp. 213–237, 1998.
- [17] C. Kirchner, M. Herty, S. Göttlich, and A. Klar, “Optimal control for continuous supply network models,” *Netw. Heterogen. Media*, vol. 1, no. 4, pp. 675–688, 2006.
- [18] O. Koroleva, M. Krstic, and G. Schmid-Schonbein, “Decentralized and adaptive control of nonlinear fluid flow networks,” *Int. J. Contr.*, vol. 16, pp. 801–818, 2006.
- [19] M. Lighthill and G. Whitham, “On kinematic waves. II. A theory of traffic flow on long crowded roads,” *Proc. Roy. Soc. London Series A, Math. Phys. Sci.*, vol. 229, no. 1178, pp. 317–345, 1955.
- [20] X. Litrico and V. Fromion, “Frequency modeling of open-channel flow,” *J. Hydraulic Eng.*, vol. 130, no. 8, pp. 806–815, 2004.
- [21] P. Malaterre, “PILOTE: Linear quadratic optimal controller for irrigation canals,” *J. Irrig. Drain. Eng.*, vol. 124, no. 4, pp. 187–194, 1998.
- [22] P. Malaterre and M. Khammash, “Controller design for a high-order 5-pool irrigation canal system,” *J. Dyn. Syst., Measure., Contr.*, vol. 125, p. 639, 2004.
- [23] P. Menon, G. Sweriduk, and K. Bilimoria, “New approach for modeling, analysis, and control of air traffic flow,” *AIAA J. Guidance, Contr., Dyn.*, vol. 27, no. 5, pp. 737–744, 2004.
- [24] P. Menon, G. Sweriduk, T. Lam, G. Diaz, and K. Bilimoria, “Computer-aided Eulerian air traffic flow modeling and predictive control,” *AIAA J. Guidance, Contr., Dyn.*, vol. 29, no. 1, pp. 12–19, 2006.
- [25] C. Meyer, *Matrix Analysis and Applied Linear Algebra*. Philadelphia, PA: Society for Industrial and Applied Mathematics, 2000.
- [26] K. Mueller, D. Schleicher, and K. D. Bilimoria, “Conflict detection and resolution with traffic flow constraints,” presented at the AIAA Conf. Guidance, Navig., Contr., Monterey, CA, 2002, AIAA Paper 2002-4445.
- [27] M. Nolan, *Fundamentals of Air Traffic Control*, 4th ed. Reading, MA: Brooks Cole, 2003.
- [28] B. Piccoli and M. Garavello, *Traffic Flow on Networks*. Springfield, MO: American Institute of Mathematical Sciences on Applied Mathematics, 2006.
- [29] R. Raffard, K. Amonlirdviman, J. Axelrod, and C. Tomlin, “An adjoint-based parameter

- identification algorithm applied to planar cell polarity signaling,” *IEEE Trans. Autom. Control (Special Issue on Systems Biology)*, vol. 53, pp. 109–121, Jan. 2008.
- [30] R. Raffard, J. Hu, and C. Tomlin, *Adjoint-Based Optimal Control of the Expected Exit Time for Stochastic Hybrid Systems*, M. Morari and Thiele, Eds. Berlin, Germany: Springer-Verlag, 2005, pp. 557–572.
- [31] R. Raffard, S. Waslander, and C. Tomlin, “Toward efficient and equitable distributed air traffic flow control,” in *Proc. 2006 Amer. Contr. Conf.*, Minneapolis, MN, Jun. 2006, pp. 5189–5194.
- [32] R. L. Raffard and C. J. Tomlin, “Second order adjoint-based optimization of ordinary and partial differential equations with application to air traffic flow,” in *Proc. Amer. Contr. Conf.*, Portland, OR, 2005, pp. 798–803.
- [33] P. I. Richards, “Shock waves on the highway,” *Oper. Res.*, vol. 4, no. 1, pp. 42–51, 1956.
- [34] S. Roy, B. Sridhar, and G. C. Verghese, “An aggregate dynamic stochastic model for air traffic control,” in *Proc. 5th USA/Eur. ATM 2003 R&D Seminar*, Budapest, Hungary, Jun. 2003.
- [35] B. Sanders and N. Katopodes, “Control of canal flow by adjoint sensitivity method,” *J. Irrig. Drain. Eng.*, vol. 125, no. 5, pp. 287–297, 1999.
- [36] B. Sridhar, T. Soni, K. Sheth, and G. Chatterji, “An aggregate flow model for air traffic management,” presented at the AIAA Conf. Guidance, Navig., Contr., Providence, RI, Aug. 2004, AIAA Paper 2004-5316.
- [37] J. C. Strikwerda, *Finite Difference Schemes and Partial Differential Equations*. Philadelphia, PA: SIAM, 2004.
- [38] I. Strub and A. Bayen, “Weak formulation of boundary conditions for scalar conservation laws: An application to highway modeling,” *Int. J. Robust Nonlinear Contr.*, vol. 16, pp. 733–748, 2006.
- [39] D. Sun and A. Bayen, “A new Eulerian-Lagrangian large-capacity cell transmission model for en route traffic,” *AIAA J. Guidance, Contr. Dyn.*, vol. 31, no. 3, pp. 616–628, 2008.
- [40] D. Sun, I. Strub, and A. Bayen, “Comparison of the performance of four Eulerian network flow models for strategic air traffic flow management,” *Netw. Hetero. Media*, vol. 2, no. 4, pp. 569–594, 2007.
- [41] C. Zhu, R. Byrd, and J. Nocedal, “L-BFGS-B: Algorithm 778: L-BFGS-B, FORTRAN routines for large scale bound constrained optimization,” *ACM Trans. Math. Software*, vol. 23, no. 4, pp. 550–560, 1997.

ABOUT THE AUTHORS

**Daniel B. Work** (Student Member, IEEE) received the B.S. degree in civil and environmental engineering from The Ohio State University, Columbus, in 2006 and the M.S. degree in civil and environmental engineering from the University of California, Berkeley, in 2007, where he is currently pursuing the Ph.D. degree in civil and environmental engineering.



His research interests include air traffic optimization, highway traffic estimation and control, and inverse modeling using mobile phones as Lagrangian sensors. He is a Research Intern on the Mobile Internet Services Systems team with Nokia Research Center Palo Alto.

Mr. Work received the Dwight David Eisenhower Transportation Fellowship from the U.S. Department of Transportation in 2008.

**Alexandre M. Bayen** (Member, IEEE) received the Engineering degree in applied mathematics from Ecole Polytechnique, France, in 1998. He received the M.S. and Ph.D. degrees in aeronautics and astronautics from Stanford University, Stanford, CA, in 1999 and 2003, respectively.



He was a Visiting Researcher at NASA Ames Research Center from 2000 to 2003. Between January and December 2004, he was Research Director of the Autonomous Navigation Laboratory, Laboratoire de Recherches Balistiques et Aerodynamiques, Ministère de la Defense, Vernon, France, where he holds the rank of Major. He has been an Assistant Professor in the Department of Civil and Environmental Engineering, University of California, Berkeley, since 2005.

Dr. Bayen received the William F. Ballhaus Prize for Outstanding Doctoral Dissertation in Aeronautics in 2004.